Progress In Electromagnetics Research B, Vol. 48, 329–346, 2013

DISORDERED FIELD PATTERNS IN A WAVEGUIDE WITH PERIODIC SURFACES

Hector Pérez-Aguilar[1, *], Alberto Mendoza-Suárez[1], Eduardo S. Tututi[1], and Ivan F. Herrera-González[2]

[1]Facultad de Ciencias Físico-Matemáticas, Universidad Michoacana de San Nicolás de Hidalgo, Av. Francisco J. Mújica S/N 58030, Morelia, Michoacán, México

[2]Instituto de Física, Benemérita Universidad Autónoma de Puebla, Apartado Postal J-48, Puebla 72570, México

Abstract—This paper considers an electromagnetic waveguide composed of two periodic, perfectly conducting, rippled surfaces. This periodic system has a band structure given by a dispersion relation that allows us characterize eigenmodes of the system. We considered the cases of both smooth and rough surfaces, using an integral numerical method to calculate field intensities corresponding to eigenmodes over a wide frequency range. Under certain conditions, the system presents disordered patterns of field intensities with smooth surfaces. We believe that the explanation of disordered patterns is the following: for smooth surfaces, the phenomenon of electromagnetic chaos; and for rough surfaces, the speckle phenomenon. Since it is well known that the surfaces of materials always have a certain degree of roughness, it can be concluded that both chaos and speckle contribute to the presence of disordered field patterns.

1. INTRODUCTION

It is now recognized that the basic random interference phenomenon underlying disordered patterns has close parallels in many other branches of physics and engineering [1]. Perhaps the earliest investigations of the properties of electromagnetic fields scattered from rough surfaces were those conducted by Lord Rayleigh [2]. It is also well known that, as a result of the interference among the distinct random contributions from the scattering centers, on scale of the

Received 5 December 2012, Accepted 28 January 2013, Scheduled 30 January 2013

* Corresponding author: Hector Pérez-Aguilar (hiperezag@yahoo.com).

optical wavelength, the scattered field pattern appears disordered, with certain granularity. This irregular pattern is best described by methods of probability theory and statistics. The physical origin of the observed granularity, now know as "laser speckle", was quickly recognized by early workers in the field [3, 4].

The study of the statistical properties of disordered systems is of fundamental importance because it leads to phenomena such as weak (enhanced backscattering) [5] and strong (Anderson) [6] localization, intensity correlations [7], and universal conductance fluctuations [8]. Furthermore, recent developments on the theory of disordered systems based upon nonlinear o models using supersymmetry theory [9] have led to the recognition that the extreme diffusive limit of disordered systems also behaves similarly to quantum chaotic systems.

One particularly important issue in this field is the attempt to identify evidence of chaos in the transport properties of ballistic systems. In fact, the magnetoresistance has been measured in chaotic and in regular cavities showing clearly distinctions in quantum transport [10]. The signature of chaos in classical transport through waveguides has also been investigated, and shows a completely different behavior on the resistivity when the system is regular or chaotic [11, 12].

This paper examines an electromagnetic waveguide composed of two periodic, perfectly conducting, rippled surfaces, taking into account the cases of both smooth and rough surfaces. Thus, this paper completes the study of the system introduced in Ref. [13]. The results of this study show that the system has many interesting properties.

The study of the transport properties of random systems has considered that disorder in the system is usually represented by impurities that are randomly distributed over the whole sample. However, it is worth mentioning that our system of a waveguide with smooth rippled surfaces can present disordered field patterns; under certain conditions, of course. This kind of systems has been the subject of several studies in recent years due to their importance in the design of antennas and rectangular waveguides for macroscopic systems [14–16] and waveguides that are related to photonic crystals, as per Ref. [13]. These systems, which constitute periodic arrays of different materials with a unit cell of dimensions of the order of the wavelength, hold the potential to develop new technologies of integrated optical circuits [17].

The geometry of waveguides with smooth rippled surfaces has been considered to constitute some billiard systems in order to study their quantum and classical transport properties [12, 18, 19]. Hence, it is important to mention that using the geometry of the proposed

system with smooth surfaces for modeling a classical waveguide, usually leads to chaotic behavior in the trajectories of the particles that are transported through it. Thus, this paper also considers the manifestation of classical chaotic dynamics in the corresponding electromagnetic system through an infinite rippled waveguide.

A disordered pattern is not enough to ensure the presence of chaos since it is difficult to distinguish between chaotic and speckle patterns [20, 21]. However, these chaotic and speckle phenomena have applications in various uses, such as coupling high pump power into chaotic double-clad EDFA's [20], mechanical models of Chua's circuit [22], cryptography based on chaotic systems [23], algorithmic trading [24], measurements of coherence [25], surface roughness [26], and displacement of an object [27], among others.

This paper is organized as follows: Section 2 introduces an integral method to calculate the field intensities of an infinite optical waveguide based on the ideas of Ref. [28]. Section 3 shows numerical results of disordered patterns in a waveguide with surfaces modeled with smooth harmonic profiles. Section 4 uses another integral method to obtain some numerical results in the case of a more realistic finite waveguide with rough surfaces. Finally, Section 5 presents our conclusions.

2. THEORETICAL APPROACH

Analysis is based on a waveguide composed of two periodic, perfectly conducting, rippled surfaces. The medium between the surfaces is vacuum. We assume translational symmetry of our system along the z-direction. The geometry of the infinite system is sketched in Figure 1(a).

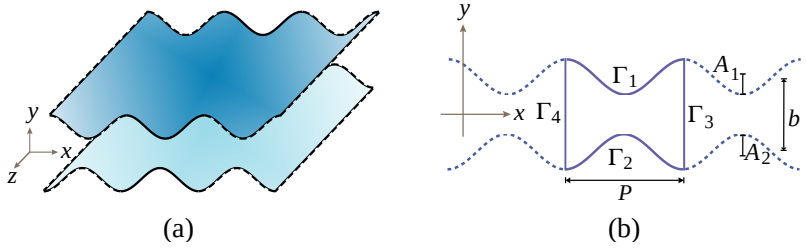

Figure 1. (a) Waveguide composed of two infinite periodic, perfectly conducting, rippled surfaces. (b) Graphic description of the infinite waveguide formed by two rippled walls in the xy-plane. The Γ contours define the unit cell of the system with periodicity in the x-direction.

In order to describe the infinite waveguide formed by two rippled walls in the xy-plane (shown in Figure 1(b)), we consider that the periodic profiles of the walls have period P, that the average width of the waveguide is given by b, and that the surface profiles can be represented by the harmonic functions $b/2 + A_1 \cos(2\pi x/P)$ (upper profile) and $-b/2 + A_2 \cos(2\pi x/P - \Delta\phi)$ (lower profile), where A_1 and A_2 represent the amplitudes and $\Delta\phi$ stands for a phase difference between the two profiles. The region enclosed by the curves Γ_1, Γ_2, Γ_3 and Γ_4 can be considered as a unit cell of the system. The set of an infinite number of unit cells is a waveguide of infinite length represented by a perfect crystal. A finite number (large enough) of unit cells is a waveguide of finite length represented by a truncated crystal (see Ref. [13]).

Let us consider the problem of finding the electromagnetic field inside the waveguide. An integral method is used that can be formulated by following the same ideas developed elsewhere [28–30]. This problem can be studied using the scalar theory by considering two complementary polarization states given the symmetry of our physical system along the z-direction. This work considers only the case of an electromagnetic field with TE polarization with E_z representing the z-component of the electric field.

It is well-known that the function $E_z(\mathbf{r})$ satisfies the Helmholtz equation

$$\nabla^2 E_z(\mathbf{r}) + \left(\frac{\omega}{c}\right)^2 E_z(\mathbf{r}) = 0, \tag{1}$$

where ω is the frequency of the electromagnetic wave, c the speed of light in vacuum, and $\mathbf{r} = x\hat{\imath} + y\hat{\jmath}$ a two-dimensional vector independent of the coordinate z.

The periodicity in the x-direction is another symmetry condition that is considered. Due to this property and the form of the differential equation Eq. (1), the Bloch theorem can be applied for the x-direction. In this way, the following expression can be derived

$$E_z(x - P, y) = \exp(-ikP)\, E_z(x, y), \tag{2}$$

where k is the one-dimensional Bloch vector.

In order to determine the electric field, first of all we have to find the dispersion relation $\omega = \omega(k)$. With this in mind, let us consider a Green's function for a two-dimensional geometry that can be used to solve the Helmholtz equation. The Green's function considered is $G(\mathbf{r}, \mathbf{r}') = i\pi H_0^{(1)}(K|\mathbf{r} - \mathbf{r}'|)$, where $H_0^{(1)}(\varrho)$ is the Hankel function of the first kind and zero order, and $K = \omega/c$. Considering the geometry of the unit cell shown in Figure 1(b) and applying the two-dimensional second Green's theorem for the functions E_z and G, we obtain the

expression

$$\frac{1}{4\pi}\oint_{\Gamma}\left[G(\mathbf{r},\mathbf{r}')\frac{\partial E_z(\mathbf{r}')}{\partial \mathbf{n}'}-\frac{\partial G(\mathbf{r},\mathbf{r}')}{\partial \mathbf{n}'}E_z(\mathbf{r}')\right]ds'=E_z\left(\mathbf{r}\right)\theta\left(\mathbf{r}\right), \quad (3)$$

being $\theta(\mathbf{r})=1$ if $\mathbf{r}$ is inside the unit cell and $\theta(\mathbf{r})=0$ otherwise. ds' is the differential arc's length, $\mathbf{n}'$ the outward normal vector to Γ, and the observation point $\mathbf{r}$ is infinitesimally separated of contour Γ outer to the unit cell. The geometry of the problem is described by representing the points along the contour Γ with Cartesian coordinates $X(s')$, $Y(s')$ as parametric functions of the arc's length s' and their derivatives $X'(s')$, $Y'(s')$, $X''(s')$ and $Y''(s')$, up to second order.

In order to solve numerically Eq. (3), we divide the curve Γ in four segments Γ_1, Γ_2, Γ_3 and Γ_4 (Fig. 1(b)) and take a sampling $X_n = X(s_n)$, $Y_n = Y(s_n)$ along the each curve. The corresponding number of points along the curves are N_1, N_2, N_3 and N_4 respectively, and $N = N_1 + N_2 + N_3 + N_4$ to the total number of points is defined. It is important to mention that the points $(X_n,\ Y_n)$ on Γ_3 must be corresponding to those on Γ_4 $(X_n - P, Y_n)$, in this way $N_3 = N_4$. Besides these considerations, we take into account the boundary condition at the perfectly conducting surfaces (with curves Γ_1 and Γ_2). Therefore, Eq. (3) can be represented numerically in terms of a homogeneous system of N algebraic equations as follows:

$$\sum_{n=1}^{N_1}L_{mn(1)}\Phi_{n(1)}+\sum_{n=1}^{N_2}L_{mn(2)}\Phi_{n(2)}+\sum_{n=1}^{N_3}L_{mn(3)}\Phi_{n(3)}$$
$$-\sum_{n=1}^{N_3}N_{mn(3)}\Psi_{n(3)}+\sum_{n=1}^{N_4}L_{mn(4)}\Phi_{n(4)}-\sum_{n=1}^{N_4}N_{mn(4)}\Psi_{n(4)}=0, \quad (4)$$

for $m = 1, 2, \ldots, N$. In Eq. (4) the source functions $\Psi_{n(3)}$ and $\Phi_{n(j)}$ represent numerically the field E_z and its normal derivative. Besides, the subscripts $n(j)$, $j = 1, 2, 3, 4$ denote the n-th point along the Γ_j contour. The matrix element $L_{mn(j)}$ and $N_{mn(j)}$ are given by [28, 29]

$$L_{mn(j)}=i\frac{\Delta s}{4}H_0^{(1)}\left(\frac{\omega}{c}d_{mn}\right)(1-\delta_{mn})+i\frac{\Delta s}{4}H_0^{(1)}\left(\frac{\omega}{c}\frac{\Delta s}{2e}\right)\delta_{mn}, \quad (5)$$

and

$$N_{mn(j)}=i\frac{\Delta s}{4}\frac{\omega}{c}H_1^{(1)}\left(\frac{\omega}{c}d_{mn}\right)\frac{D_{mn}}{d_{mn}}(1-\delta_{mn})+\left(\frac{1}{2}+\frac{\Delta s}{4\pi}D'_n\right)\delta_{mn}, \quad (6)$$

where

$$d_{mn} = \sqrt{(X_m-X_n)^2+(Y_m-Y_n)^2}, \quad (7)$$

$$D_{mn} = -Y'_n\left(X_m-X_n\right)+X'_n\left(Y_m-Y_n\right), \quad (8)$$

$$D'_n = X'_n Y''_n - X''_n Y'_n. \tag{9}$$

$H_1^{(1)}(\varrho)$ is the Hankel's function of first kind and first order. The function $\delta_{mn}^{(j)}$ represents the Kronecker's delta and Δs is the arc's length between two consecutive points of a given curve. In Eqs. (8) and (9), we have defined $X'_n = X'(s)|_{s=s_n}$, $X''_n = X''(s)|_{s=s_n}$, and so forth. For simplicity we have omitted the contour index (j) but it must be implicitly understood that $n = n(j)$ wherever it appears in Eqs. (5)–(9).

By applying Eq. (2) we obtain the equations $\Psi_n^{(4)} = \exp(-ikP)\Psi_n^{(3)}$, and $\Phi_n^{(4)} = -\exp(-ikP)\Phi_n^{(3)}$. The minus sign appearing in last equation results because the normals to corresponding points at Γ_3 and Γ_4 have opposite directions. Using these equations, we obtain

$$\sum_{n=1}^{N_1} L_{mn(1)}\Phi_{n(1)} + \sum_{n=1}^{N_2} L_{mn(2)}\Phi_{n(2)} + \sum_{n=1}^{N_3} \left(L_{mn(3)} - \exp\left(-ikP\right) L_{mn(4)}\right)$$
$$\times \Phi_{n(3)} - \sum_{n=1}^{N_3} \left(N_{mn(3)} + \exp\left(-ikP\right) N_{mn(4)}\right) \Psi_{n(3)} = 0, \tag{10}$$

with $m = 1, 2, \ldots, N$. Eq. (10) constitutes a linear system that has an associated representative matrix, M_{mn}, that depends on the frequency ω and the Bloch vector k. Since the equation system is homogeneous, a nontrivial solution can be obtained if the determinant of such matrix defined as

$$D\left(k, \omega\right) = \ln\left(\left|\det\left(M\right)\right|\right) \tag{11}$$

is zero. Numerically this function (Eq. (11)) presents local minimum points that will give us the numeric dispersion relation $\omega = \omega(k)$.

For our purposes, this work requires analyzing the intensity, defined by $E_z^* E_z$, in a unit cell. In order to calculate it for a eigenmode at a given point $(k,\ \omega)$, one must consider the dispersion relation obtained numerically by the use of a homogeneous equation system. Additional details of the numerical method employed can be found in Ref. [13].

3. CLASSICAL CHAOTIC BEHAVIOR AND ITS ELECTROMAGNETIC COUNTERPART

We mentioned above that the geometry of the proposed system herein has been considered in order to study its quantum and classical transport properties [12, 18, 19]. According to this study, the system

analyzed could present some signatures of electromagnetic wave chaos for certain parameters.

We shall calculate certain eigenmodes in the unit cell to observe some traces of the chaotic behavior of our system. But first the corresponding classical system must be examined to demonstrate the presence of chaos.

Let us consider the corresponding billiard-ball model of our infinite waveguide with rippled walls (see Figure 1(b)) with the following geometric values $b = 1.5\,\mu\text{m}$, $\Delta\phi = \pi/2$ and $P = 2\pi\,\mu\text{m}$. The dynamics of the system can be qualitatively described by the Poincaré plots, which are determined by the set of points $(x_n, p_n = \cos\theta_n)$. Here, x_n, θ_n are the x-coordinate and the angle that the trajectory of the particle makes with the x-axis just after the n-th collision with the upper wall. In order to obtain all possible orbits in the Poincaré plots, several initial conditions of the particle in the phase space need to be considered and due to the periodicity of the channel, the structure of the Poincaré section is periodic with period 2π. For this reason, we choose the x-interval $[\pi, 3\pi]$ to study the dynamics of the system. The Poincaré plots exhibit a generic transition to chaos as the ripple amplitude is increased (the reader is referred to [12] for a detailed discussion of this phenomenon). Here, we restrict our approach to just two cases. The first is the flat channel ($A = 0$), where the dynamics of the particle is regular, as shown in Figure 2(a). The second corresponds to a channel with $A = 0.4b$; here the system presents mixed dynamics (the dynamics of the particle may be regular or chaotic depending on its initial conditions), as shown in Figure 2(b).

We have shown that in the classical channel, mixed chaos phenomenon is presented with the parameters used to obtain Figure 2(b). Thus, using the geometry of the proposed system for

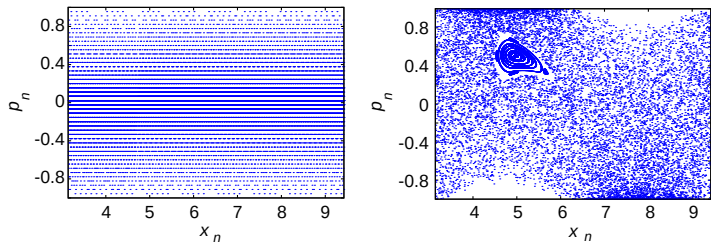

Figure 2. Poincaré plots for the narrow channel ($b = 1.5\,\mu\text{m}$) with a phase difference $\Delta\phi = \pi/2$ and amplitudes, (a) $A = 0.0$, and (b) $A = 0.4b$.

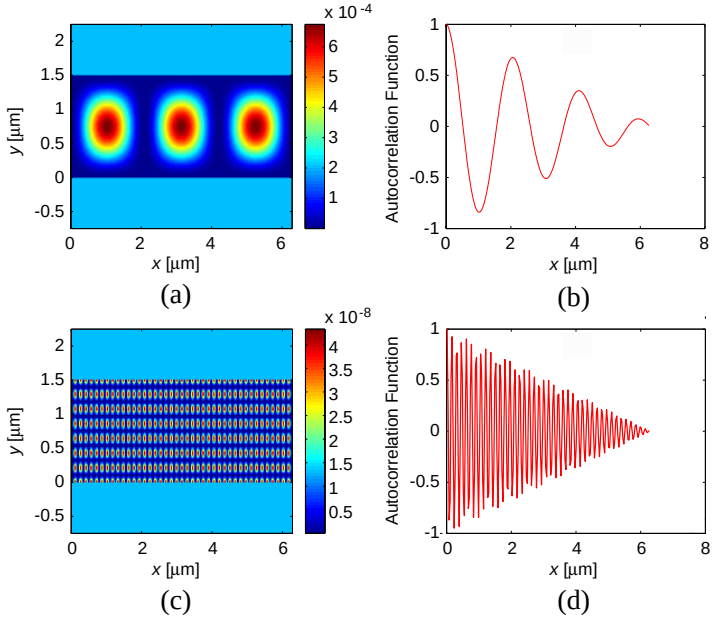

Figure 3. Field intensities in a flat waveguide with $b = 1.5\,\mu\text{m}$ for the lower frecuency (a) $\nu = 123.203\,\text{THz}$ and the higher frequency (c) $\nu = 5720.244\,\text{THz}$. The corresponding autocorrelation functions are shown in (b) and (d), respectively.

modeling a classical waveguide, usually leads to the appearance of chaotic phenomena. Likewise, chaotic behavior must also appear in the study of the electromagnetic waveguide. This can be shown by examining the case of high frequencies.

Now, we shall to consider our waveguide, illustrating some of the characteristics of electromagnetic wave chaos as follows: by depicting intensity of eigenmodes, normalized in the region defined by the unit cell, for the cases of low and high frequencies. Also, the corresponding autocorrelation functions will be shown, as they have been found to be important in the interpretation of electromagnetic wave chaos [20].

Figures 3(a) and 3(c) show the intensities inside a flat waveguide with $b = 1.5\,\mu\text{m}$. We obtained the figures for both the low frequency $\nu = 123.203\,\text{THz}$ [Figure 3(a)], and the high frequency $\nu = 5720.244\,\text{THz}$ [Figure 3(c)], using the Bloch vector $k = 0$. The corresponding autocorrelation functions are shown in Figures 3(b) and 3(d), respectively. We consider the correlation length l defined as the standard deviation of the spatial autocorrelation. For the lower

frequency, the correlation length was $l = 0.4133$, while for the higher frequency it was $l = 0.4123$. In the case of a waveguide with flat walls, no chaos phenomenon appears. This is a straightforward statement and one easily to understand. As a result, similar values for the correlation lengths were obtained.

In order to make reliable calculations in the case of high frequencies, it is necessary to use small discretization intervals. Due to numerical approximations involved, $\Delta s = c/20\nu_{\max} \approx 0.0026\,\mu\text{m}$ was used. This value produced a good resolution in our calculations, which was then verified by comparing the numerical results with the corresponding analytical results for the flat waveguide.

Figures 4(a) and 4(c) show the intensities in an infinite rippled waveguide with the parameters: $P = 2\pi\,\mu\text{m}$, $b = 1.5\,\mu\text{m}$, $\Delta\phi = \pi/2$, and $A = 0.4b$. We obtained the figures for both the low frequency $\nu = 82.771\,\text{THz}$ [Figure 4(a)], and the high frequency $\nu = 5684.344\,\text{THz}$ [Figure 4(c)], using the Bloch vector $k = 0$. The

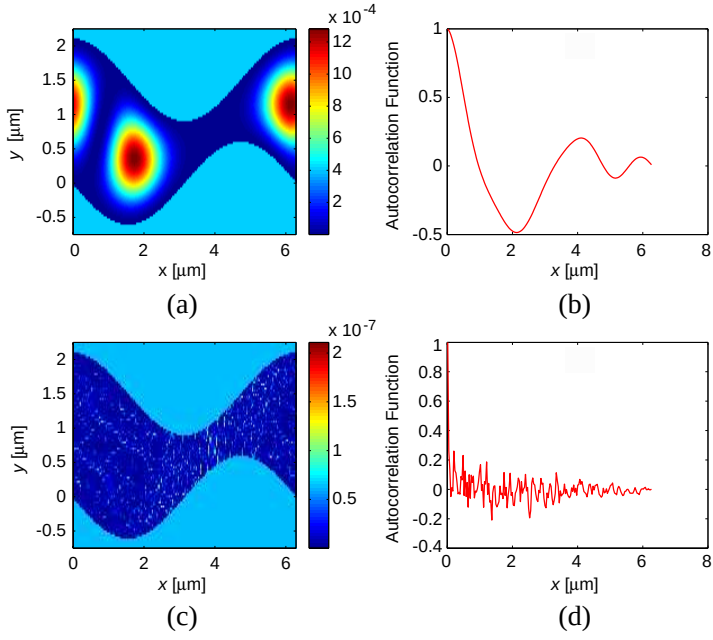

Figure 4. Field intensities in an infinite rippled waveguide with $b = 1.5\,\mu\text{m}$, $A = 0.4b$ and $\Delta\phi = \pi/2$ for the lower frequency (a) $\nu = 82.771\,\text{THz}$ and the higher frequency (c) $\nu = 5684.344\,\text{THz}$. The corresponding autocorrelation functions are shown in (b) and (d), respectively.

corresponding autocorrelation functions are shown in Figures 4(b) and 4(d), respectively. For the lower frequency, the correlation length was $l = 0.3241$, while for the higher frequency it was $l = 0.0977$.

Upon comparing the correlation lengths obtained, the latter case had a small value for the parameter l. We believe this is a manifestation of electromagnetic wave chaos, since in this regime led us to think that the intensity of the eigenmode is an uncorrelated random variable as a function of a point $(x,\ y)$ in the unit cell. In this case, the intensity cannot be represented by a function with smooth variations that give rise to the appearance of disordered peaks. This effect is also a characteristic of quantum chaos (see Ref. [18]). A disordered pattern is not enough to ensure the presence of chaos; nevertheless, the corresponding classical channel obviously presents chaos behavior, and this is our main argument.

4. FINITE ROUGH WAVEGUIDE

In the previous section, Figure 4(c) was included to show some signatures of chaotic behavior using the intensity of the eigenmode in the real space. Other results are shown in a similar way in Ref. [20, 21]. It is well known that the surfaces of materials always have a certain degree of roughness, and that is difficult to distinguish chaotic patterns from speckle patterns [20]. This motivated us to present some calculations for waveguides with rough surfaces that give rise to intensities with disordered patterns; patterns that are similar to those shown in Figure 4(c). This makes it possible to present a system in which chaos and speckle appear simultaneously.

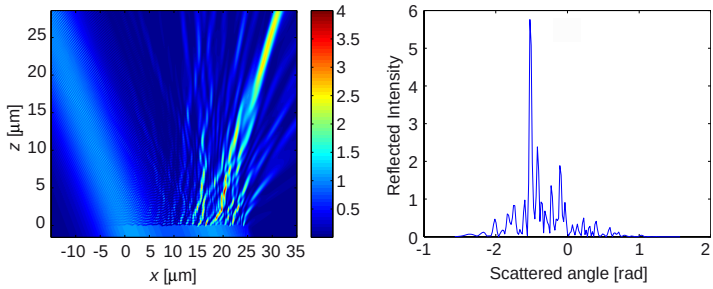

Figure 5. (a) Field intensity above a one-dimensional rough surface with rms height $\delta = 0.08$ and correlation length $a = 0.4$. (b) Speckle pattern in far field.

The speckle effect occurs if the size of surface roughness is around of the wavelength of the incident beam [31]. With this in mind, one can properly choose the parameters for the numerical simulations. As an example, Figure 5(a) shows the speckle pattern (field intensity) by a one-dimensional perfectly conducting rough surface. The surface is illuminated at 30 degrees by a Gaussian beam with a wavelength $\lambda = 0.6120\,\mu\text{m}$. The roughness profile is a certain realization of an ensemble used to model a random surface with Gaussian statistics. The ensemble has a mean profile that corresponds to a flat surface. The theoretical parameters assumed in obtaining these results were the length correlation $a = 0.4\,\mu\text{m}$ and the rms height $\delta = 0.08\,\mu\text{m}$ for the frequency $\nu = 490.1940\,\text{THz}$ [32]. The corresponding speckle pattern in far field zone is shown in Figure 5(b).

As a consequence of the surface roughness on the scale of the optical wavelength, the various wavefronts are added with markedly different phases, resulting in a highly complex pattern of interference. The image of this pattern [Figure 5(a)] is found to have threads (or granular) appearance with a multitude of bright and dark threads (or spots). This calculation also makes it possible to see the scattered field intensity in the far field zone, which appears as a curve with very abrupt changes [Figure 5(b)].

Now, another of our interests was to obtain speckle patterns in a waveguide formed by rough surfaces. For this case, it is necessary to consider a finite waveguide composed of two periodic, perfectly conducting, rippled surfaces illuminated by an incident electromagnetic wave, as shown in Figure 6(a). To approach this problem, some considerations must be assumed and we shall bear in mind it in the xy-plane. Since the size of the system is finite, to avoid edge effects we illuminate it with a tapered Gaussian beam whose intercept with the plane of the channel has a half-width g. This parameter must be smaller than the total length of the system $L_y = 2l + b$, but much larger than the width of the aperture b (see Figure 6(b)).

Under these considerations, the incident field can be expressed in terms of its angular spectrum $A(q, k_\parallel)$

$$\Psi_{inc}(x, y) = \int_{-\omega/c}^{\omega/c} \frac{dq}{2\pi} A(q, k_\parallel) \exp\{i\,[qx - \alpha_0(q)y]\}, \tag{12}$$

where $\alpha_0(q) = [(\omega/c)^2 - q^2]^{1/2}$ with $\Re e\,\alpha_0(q) > 0$ and $\Im m\,\alpha_0(q) > 0$. In this work we choose

$$A(q, k_\parallel) = \sqrt{\pi} g \exp\left\{-g^2(q - k_\parallel)^2/4\right\}, \tag{13}$$

where the parameter $k_\parallel = (\omega/c)\sin\theta_0$, being θ_0 the angle of incidence

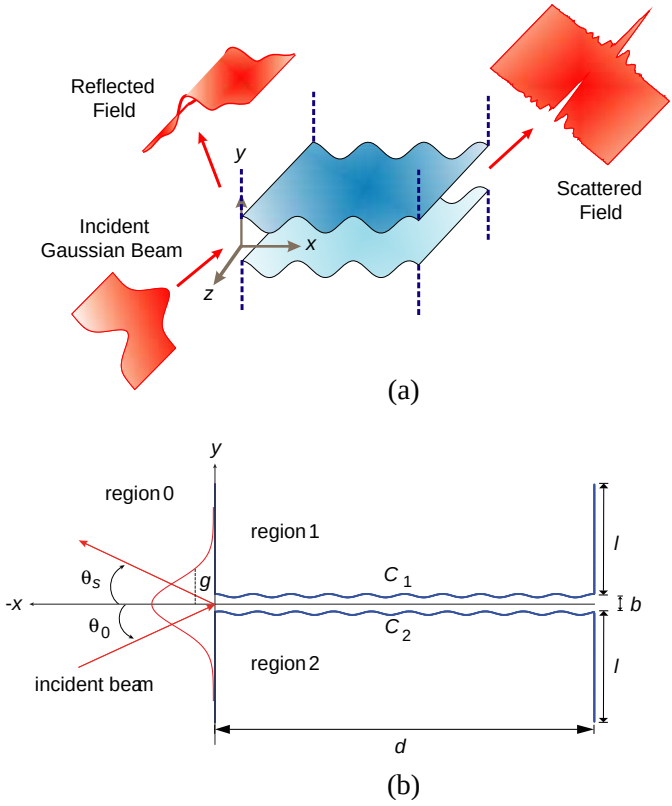

Figure 6. (a) Waveguide composed of two finite periodic, perfectly conducting, rippled surfaces illuminated by a Gaussian beam. The reflected and transmitted field patterns are shown. (b) Schematic description of the waveguide of width b and length d with rippled surfaces in the xy-plane is illuminated by a Gaussian beam in region 0. Regions 1 and 2 constitute the perfect conductor. The $1/e$ half-width of the modulus of the incident Gaussian beam projected on the plane $x = 0$ is g. The angles of incidence θ_0 and scattering θ_s for reflection are also shown.

(see Figure 6(b)). Additional details of the numerical method can be found in Refs. [13, 33].

A field speckle pattern by two perfectly conducting rough surfaces is shown in Figure 7. The waveguide was illuminated at normal incidence by a Gaussian beam with a wavelength $\lambda = 0.3112\,\mu$m. The theoretical parameters used in obtaining these results were $a = 0.4712$ and $\delta = 0.075$ for the frequency $\nu = 964.0289\,$THz. The roughnesses

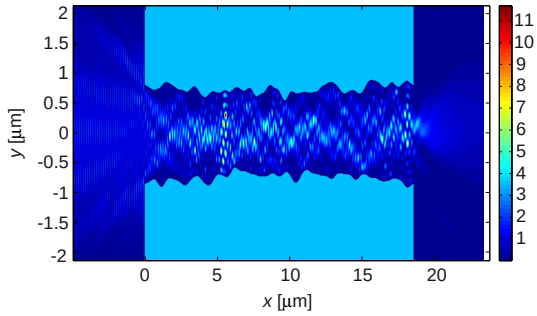

Figure 7. Field speckle pattern produced by two perfectly conducting rough surfaces with $a = 0.4712$ and $\delta = 0.075$ for the frequency $\nu = 964.0289\,\text{THz}$.

belong to an ensemble whose mean profiles correspond to flat surfaces.

Figure 7 also shows a disordered pattern with the appearance of a multitude of bright and dark spots. This irregular pattern is formed by the interference among scattered fields produced by the two rough surfaces on scale of an optical wavelength, as was shown for only a rough surface [Figure 5(a)]. Obviously, the disorder is seen here a consequence of the speckle phenomenon.

In the previous section, we considered a waveguide of infinite length, a property that is essential to ensuring that our system has a well-defined dispersion relation $\omega = \omega(k)$. The numerical method used to calculate intensities assumes a perfect periodicity. However, a realistic waveguide always has a finite length. A finite number (large enough) of unit cells is a waveguide of finite length that can be represented by a truncated crystal. Fortunately, only a few periods are suffice to obtain some of the main results for the perfectly periodic waveguide [13]. It is important to take into account specific eigenmodes of the infinite waveguide for the proper selection of parameters for the case of finite waveguides.

In order to study how the effects of speckle change the intensity pattern of a waveguide with rippled surfaces, we consider surfaces with both smooth and rough profiles. Figure 8(a) shows the field intensity in a finite waveguide with smooth surfaces.The waveguide has the following parameters $d = 20\pi\,\mu\text{m}$, $P = 2\pi\,\mu\text{m}$, $b = 1.5\,\mu\text{m}$, $\Delta\phi = \pi/2$ and $A = 0.1b$. The waveguide was illuminated at normal incidence by a Gaussian beam with a frequency $\nu = 963.4667\,\text{THz}$ [Figure 8(a)]. Considering a waveguide with rough surfaces, Figure 8(b) shows the corresponding field intensity. The rough profiles [in Figure 8(b)] were obtained by adding the smooth profiles [Figure 8(a)] to the rough

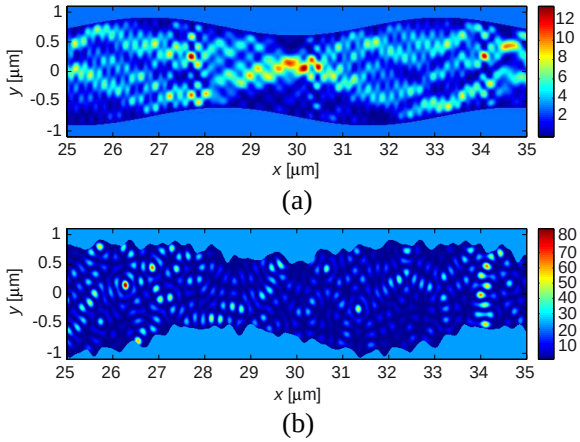

Figure 8. Field intensities in (a) a finite smooth waveguide with $b = 1.5\,\mu\text{m}$, $A = 0.1b$ and $\Delta\phi = \pi/2$ for $\nu = 963.4667\,\text{THz}$ and in (b) a finite rough waveguide with $a = 0.025P$ and $\delta = 0.05b$ for $\nu = 960.4062\,\text{THz}$.

profiles used in Figure 7. In this case, Figure 8(b) was obtained for the frequency $\nu = 960.4062\,\text{THz}$. In the remainder of this paper, only one section of the finite waveguide of length $d = 20\pi\,\mu\text{m}$ is sketched, in order to achieve a clearer representation.

It can be seen clearly that the pattern in Figure 8(a) is disturbed due to surface roughness. Of course, the disorder pattern in Figure 8(b) is a consequence of the speckle phenomenon.

Finally, let us consider a system in which the effects of both chaos and speckle contribute to the appearance of disordered field patterns. To obtain the presence of chaos phenomenon it is necessary to realize calculations for high frequencies. Figure 9 presents the field intensity associated with a finite waveguide with rough surfaces of length $d = 20\pi\,\mu\text{m}$. The surfaces profiles were obtained analogously to the case of Figure 8. The parameters used were: $b = 1.5\,\mu\text{m}$, $A = 0.4b$, $\Delta\phi = \pi/2$, $a = 0.025P$ and $\delta = 0.05b$. For this case, the frequency $\nu = 3822.2316\,\text{THz}$ was used.

We believe that the disordered pattern in Figure 9 is the result of the combination of chaos and speckle, though these two phenomena are mixed in a way that renders them indistinguishable. The autocorrelation function associated with the field intensity in Figure 9 is similar to the function shown in Figure 4(d). For this case, a correlation length of $l = 0.0451$ was obtained. The disorder in Figures 4(c) and 9 was compared using the corresponding

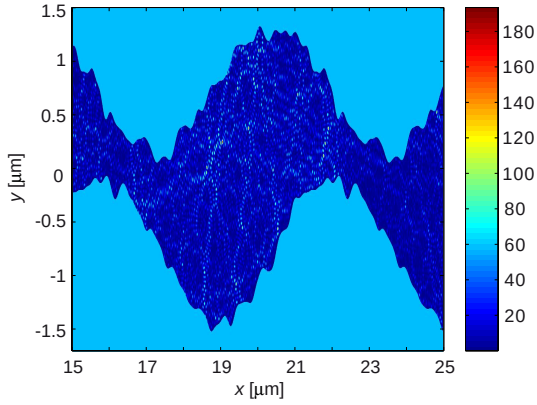

Figure 9. Field intensity pattern in a finite rough rippled waveguide with $b = 1.5\,\mu\text{m}$, $A = 0.4b$, $\Delta\phi = \pi/2$ for the frequency $\nu = 3822.2316\,\text{THz}$.

autocorrelations given a similar behavior, since the values of the correlation lengths were almost identical.

It is noteworthy that the numerical calculations realized to obtain these figures show that the energy conservation is satisfied above 95%. This comment is important because the disordered that appears in Figure 9 could be interpreted as numerical instability, but this is not the case. Our experience with integral methods applied to a variety of systems allow us to affirm that, if numerical instabilities occur, then the energy conservation would be violated at a high percentage.

5. CONCLUSIONS

An integral numerical method was applied to study a waveguide composed of two periodic, perfectly conducting, rippled surfaces. It is important to note that for certain conditions, disordered patterns of field intensities in waveguides with smooth surfaces were obtained. In general, disordered patterns are associated with disordered systems, whereby this result contrasts with this belief and it is interesting for possible applications.

The corresponding classical model of our electromagnetic system presents a chaotic behavior under certain conditions. This is our main argument in terms of interpreting some of our results as manifestations of electromagnetic wave chaos. The signature of the classical chaotic behavior in the electromagnetic model is manifested in the spatial statistical properties of the probability density. In particular, the

correlation length of the autocorrelation function goes to zero when the corresponding classical system is chaotic.

It is also possible to obtain a disordered pattern for low frequencies by the effect of roughness that produces a speckle pattern. This allows us to extend the frequency range for obtaining disordered patterns.

Since the surfaces of materials always have a certain degree of roughness, it can be concluded that both chaos and speckle contribute to the presence of disordered field patterns.

ACKNOWLEDGMENT

The authors wish to express their gratitude to Consejo Nacional de Ciencia y Tecnología (México) for financial support through grant 54770, to the Coordinación de la Investigación Científica at the Universidad Michoacana de San Nicolás de Hidalgo, and to the Red de Cuerpos Académicos PROMEP-SEP (FOFM-2008).

REFERENCES

1. Shen, J.-T. and S. Fan, "Strongly correlated two-electron transport in a quantum waveguide having a single Anderson impurity," *New J. Phys.*, No. 11, 113024, 2009.
2. Rayleigh, L., "On the resultant of a large number of vibrations of the same pitch and of arbitrary phase," *Phil. Mag.*, Vol. 10, 73–78, 1880.
3. Rigden, J. D. and E. I. Gordon, "The granularity of scattered optical maser light," *Proc. IRE*, Vol. 50, 2367–2368, 1962.
4. Oliver, B. M., "Sparkling spots and random diffraction," *Proc. IEEE*, Vol. 5, 220–221, 1963.
5. Sheng, P., *Scattering and Localization of Classical Waves in Random Media,* World Scientific Publishing, Singapore, 1990.
6. Anderson, P. W., "Absence of diffusion in certain random lattices," *Phys. Rev. B*, Vol. 109, No. 5, 1492–1505, 1958.
7. Michel, T. R. and K. A. O'Donnell, "Angular correlation functions of amplitudes scattered from a one-dimensional, perfectly conducting rough surface," *J. Opt. Soc. Am. A*, Vol. 9, No. 8, 1374–1384, 1992.
8. Webb, R. A., S. Washburn, C. P. Umbach, and R. B. Laibowitz, "Observation of h/e Aharonov-Bohm oscillations in normal-metal rings," *Phys. Rev. Lett.*, Vol. 54, No. 25, 2696–2699, 1985.
9. Mirlin, A. D., A. Müller-Groeling, and M. R. Zirnbauer,

"Conductance fluctuations of disordered wires: Fourier analysis on supersymmetric spaces," *Ann. Phys.*, Vol. 236, 325–373, 1994.

10. Chang, A. M., H. U. Baranger, L. N. Pfeiffer, and K. W. West, "Weak localization in chaotic versus nonchaotic cavities: A striking difference in the line shape," *Phys. Rev. Lett.*, Vol. 73, No. 15, 2111–2114, 1994.
11. Luna-Acosta, G. A., A. A. Krokhin, M. A. Rodríguez, and P. H. Hernández-Tejeda, "Classical chaos and ballistic transport in a mesoscopic channel," *Phys. Rev. B*, Vol. 54, No. 16, 11410–11416, 1996.
12. Herrera-González, I. F., G. Arroyo-Correa, A. Mendoza-Suárez, and E. S. Tututi, "Study of the resistivity in a channel with dephased ripples," *Int. J. Mod. Phys. B*, Vol. 25, 683–698, 2011.
13. Mendoza-Suárez, A., H. Pérez-Aguilar, and F. Villa-Villa, "Optical response of a perfect conductor waveguide that behaves as a photonic crystal," *Progress In Electromagnetics Research*, Vol. 121, 433–452, 2011.
14. Zhang, G. G., H. Zhang, Z. L. Yuan, Z. M. Wang, and D. Wang, "A novel broadband E-plane omni-directional planar antenna," *Journal of Electromagnetic Waves and Applications*, Vol. 24, Nos. 5–6, 663–670, 2010.
15. Ye, H., H. Wang, S. P. Yeo, and C. Qiu, "Finite-boundary bowtie aperture antenna for trapping nanoparticles," *Progress In Electromagnetics Research*, Vol. 136, 17–27, 2013.
16. Sanchez-Escuderos, D., M. Ferrando-Bataller, J. I. Herranz, and M. Baquero-Escudero, "Optimization of the E-plane loaded rectangular waveguide for low-loss propagation," *Progress In Electromagnetics Research*, Vol. 135, 411–433, 2013.
17. Inoue, K. and K. Ohkata, *Photonic Crystals*, Springer, Germany, 2004.
18. Luna-Acosta, G. A., K. Na, L. E. Reichl, and A. Krokhin, "Band structure and quantum Poincaré sections of a classically chaotic quantum rippled channel," *Phys. Rev. E*, Vol. 53, No. 4, 3271–3283, 1996.
19. Herrera-González, I. F., H. I. Pérez-Aguilar, A. Mendoza-Suárez, and E. S. Tututi, "Heat conduction in systems with Kolmogorov-Arnold-Moser phase space structure," *Phys. Rev. E*, Vol. 86, No. 3, 031138-1–031138-9, 2012.
20. Doya, V., O. Legrand, and F. Mortessagne, "Light scarring in an optical fiber," *Phys. Rev. Lett.*, Vol. 88, No. 1, 014102–014105, 2002.

21. Wilkinson, P. B., T. M. Fromhold, R. P. Taylor, and A. P. Micolich, "Electromagnetic wave chaos in gradient refractive index optical cavities," *Phys. Rev. Lett.*, Vol. 86, No. 24, 5466–5469, 2001.
22. Awrejcewicz, J. and M. L. Calvisi, "Mechanical models of Chua's circuit," *Int. J. Bif. and Chaos*, Vol. 12, No. 4, 671–686, 2002.
23. Yang, T., C. W. Wu, and L. O. Chua, "Impulsive stabilization for control and synchronization of chaotic systems: Theory and application to secure communication," *IEEE Trans. Circuits Syst. — I*, Vol. 44, No. 10, 976–988, 1997.
24. Williams, B. and J. Williams, *Trading chaos: Maximize Profits with Proven Technical Techniques*, Wiley, New York, 2004.
25. Asakura, T., H. Fuji, and K. Murata, "Measurement of spatial coherence using speckle patterns," *Opt. Acta*, Vol. 19, 273, 1972.
26. Crane, R. B., "Use of a laser-produced speckle pattern to determine surface roughness," *J. Opt. Soc. Am.*, Vol. 60, No. 12, 1658–1663, 1970.
27. Tiziani, H. J., "Analysis of mechanical oscillations by speckling," *Appl. Opt.*, Vol. 11, No. 12, 2911–2917, 1972.
28. Mendoza-Suárez, A., F. Villa-Villa, and J. A. Gaspar-Armenta, "Numerical method based on the solution of integral equations for the calculation of the band structure and reflectance of one- and two-dimensional photonic crystals," *J. Opt. Soc. Am. B*, Vol. 23, No. 10, 2249–2256, 2006.
29. Mendoza-Suárez, A., F. Villa-Villa, and J. A. Gaspar-Armenta, "Band structure of two-dimensional photonic crystals that include dispersive left-handed materials and dielectrics in the unit cell," *J. Opt. Soc. Am. B*, Vol. 24, No. 12, 3091–3098, 2007.
30. Villa-Villa, F., J. A. Gaspar-Armenta, and A. Mendoza-Suárez, "Surface modes in one dimensional photonic crystals that include left handed materials," *Journal of Electromagnetic Waves and Applications*, Vol. 21, No. 4, 485–499, 2007.
31. Goodman, J. W., *Speckle Phenomena in Optics: Theory and Applications,* Roberts & Co., USA, 2007.
32. Leskova, T. A., A. A. Maradudin, "Multiple-scattering effects in angular intensity correlation functions," *Light Scattering and Nanoscale Surface Roughness*, A. A. Maradudin (ed.), Springer-Verlag, New York, 2007.
33. Pérez, H. I., E. R. Méndez, C. I. Valencia, and J. A. Sánchez-Gil, "On the transmission of diffuse light through thick slits," *J. Opt. Soc. Am. A*, Vol. 26, No. 4, 909–918, 2009.